Title

CHACTERIZATION OF CHAOTIC INSTABILITIES IN AN ELECTRON-HOLE PLASMA IN GERMANIUM

Authors

Held, G.A.
Jeffries, C.D.

Publication Date

1985-10-01

Lawrence Berkeley Laboratory
UNIVERSITY OF CALIFORNIA

Materials & Molecular Research Division

Presented at the International Workshop on Dimensions and Entropies in Chaotic Systems, Pecos River, NM, September 11-16, 1985; and published in the Proceedings

CHARACTERIZATION OF CHAOTIC INSTABILITIES IN AN ELECTRON-HOLE PLASMA IN GERMANIUM

G.A. Held and C.D. Jeffries

October 1985

Prepared for the U.S. Department of Energy under Contract DE-AC03-76SF00098

DISCLAIMER

To appear in the Proceedings of the International Workshop on Dimensions and Entropies in Chaotic Systems at Pecos River, NM, 11-16 Sept. 1985 (Springer-Verlag), edited by G. Mayer-Kress.

LBL-20526

CHARACTERIZATION OF CHAOTIC INSTABILITIES IN AN ELECTRON-HOLE PLASMA IN GERMANIUM*

G. A. Held and C. D. Jeffries

Department of Physics, University of California, Berkeley, CA 94720

and

Materials and Molecular Research Division, Lawrence Berkeley Laboratory, Berkeley, CA 94720

October 1985

*This work was supported by the Director, Office of Energy Research, Office of Basic Energy Sciences, Materials Sciences Division of the U.S. Department of Energy under Contract No. DE-AC03-76SF00098.

Characterization of Chaotic Instabilities in an Electron-Hole Plasma in Germanium

G. A. Held and C. D. Jeffries

Department of Physics and Lawrence Berkeley Laboratory, University of California, Berkeley, CA 94720, USA

Abstract

Helical instabilities in an electron-hole plasma in Ge in parallel dc electric and magnetic fields are known to exhibit chaotic behavior. By fabricating probe contacts along the length of a Ge crystal we study the spatial structure of these instabilities, finding two types: (i) spatially coherent and temporally chaotic helical density waves characterized by strange attractors of measured fractal dimension $d \sim 3$, and (ii) beyond the onset of spatial incoherence, instabilities of indeterminately large fractal dimension $d \geqslant 8$. In the first instance, calculations of the fractal dimension provide an effective means of characterizing the observed chaotic instabilities. However, in the second instance, these calculations do not provide a means of determining whether the observed plasma turbulence is of stochastic or of deterministic (i.e., chaotic) origin.

1. Introduction

It is by now well established that the onset of turbulence in a wide range of physical systems can be characterized by low-dimensional chaotic dynamics.[1] That is, the evolution of these systems corresponds to motion in phase space along trajectories confined to a strange (fractal) attractor.[2] Experimentally, it is often difficult to distinguish between deterministic chaos and stochastic noise – both are characterized by broad spectral peaks. To establish that experimentally observed behavior is indeed chaotic, it is necessary to examine the structure of the attractor itself. This requires methods of data reduction designed specifically to identify and characterize low-dimensional chaotic attractors. These include the construction of phase portraits, Poincaré

sections, return maps, and bifurcation diagrams. In those cases where the chaotic behavior is characterized by an attractor of dimension greater than approximately 2.5, even these methods of analysis cannot distinguish between chaos and stochastic noise; the fractal structure becomes too dense to be discerned through visual inspection of a two-dimensional projection of a Poincaré section. In such instances, one must calculate quantitative measures of chaos Such as fractal dimensions,[3] Lyapunov exponents,[4] and metric entropy[5] of the attractor. In this paper we present the results of our efforts to calculate fractal dimensions as a means of identifying and characterizing chaos in helical instabilities of an electron-hole (e-h) plasma in germanium (Ge).

Spontaneous current oscillations in an e-h plasma in a dc electric field E_0 and a parallel dc magnetic field B_0 are known to be the result of an unstable, travelling, screw-shaped helical density wave.[6,7] Held, Jeffries, and Haller[8] have found that when this instability is strongly excited by an increasing electric field, it will undergo both period-doubling and quasiperiodic transitions to low-dimensional chaos. Experimentally, we vary the applied dc fields and record the dynamical variables I(t), the total current passing through the sample, and V(t), the voltage across it. By forming probe contacts along the length of our crystals, we are also able to monitor the local variations in plasma density.

We have found two distinct types of behavior: (i) an essentially spatially coherent and temporally chaotic plasma density wave characterized by an attractor of fractal dimension $d \sim 3$, and (ii) a spatially incoherent wave with an immeasurably large fractal dimension $d > 8$. Further, as the applied electric field E_0 is increased, we observe a transition between these two states – characterized by a partial loss of spatial order and a jump in the fractal dimension. While the increase in fractal dimension from $d \sim 3$ to $d > 8$ is somewhat abrupt ($\Delta E_0/E_0 \sim 0.05$), the breakup of spatial order occurs gradually. It is physically reasonable that the onset of spatial incoherence (which increases the number of available degrees of freedom) would result in an increased fractal dimension. However, we cannot firmly establish that the onset of spatial disorder is *coincident* with the observed jump in fractal dimension; the possibility that these two events occur at comparable fields and yet are not directly related cannot be completely excluded.

The methods by which we determined that case (i) corresponds to a temporally chaotic, spatially coherent density wave are described in detail elsewhere.[9] We present here a discussion of the methods which we have used to determine the fractal dimension of the attractors associated with such instabilities. Following that, we discuss the difficulties which we have encountered in attempting to characterize spatially incoherent instabilities in the context of chaotic dynamics.

2. Experimental Procedures

Our experiments are performed on a $1 \times 1 \times 1\ mm^3$ sample cut from a large single crystal of n-type Ge with a net donor concentration $N_D \sim 3.7 \times 10^{12} cm^{-3}$.[8] A lithium-diffused n^+ contact (electron injecting) and a boron-implanted p^+ contact (hole injecting) were formed on opposite $1 \times 1\ mm^2$ ends. Phosphor-implanted n^+ contacts were formed on two opposite $1 \times 10\ mm^2$ faces. Using photolithography, we etched onto these two faces a pattern of eight pairs of contacts 0.5 mm wide and spaced by 1 mm along the length of the sample. The voltage $V_i(t)$ across a pair of these contacts is a measure of the local variation in plasma density.[7] The sample was lapped, etched, and then stored in dry air for 72 hours to allow the surfaces to passivate.

When taking data, the sample is cooled to 77 K in liquid N_2 and connected in series with a $100-\Omega$ resistance and a variable dc voltage, which both generates the e-h plasma via double injection and creates the dc electric field E_0. The applied voltage V_0, the applied magnetic field B_0, and the angle between the two fields θ comprise our control parameters; typically $\theta = 0 \pm 3°$. In practice, we fix B_0 and θ and sweep V_0, while recording the dynamical variables I(t), V(t), and $V_i(t)$, which characterize the plasma behavior.

3. Low-Dimensional Attractors – Transitions to "Weak" Turbulence

In different regions of parameter space (V_0, B_0, θ) different types of transitions to turbulence are observed. For our system we make the operational definition that a transition to "weak" turbulence is one in which the transition from periodicity to chaos is followed by a transition back to periodicity as V_0 is increased further. All such transitions that we have observed occur over a small range (i.e., ~ 1 V) of V_0, and in all such chaotic states there exists at least one fundamental peak which stands out clearly above the broad-band "noise" level of the power spectrum.

For several different values of B_0 we have observed quasiperiodic transitions to weak turbulence: as V_0 is increased, the onset of a quasiperiodic state (simultaneous oscillations at two incommensurate frequencies) is followed by a transition to chaos. The power spectra for one such sequence, taken at $B_0 = 11.15$ kGauss, is shown starting in figure 1(a) with $V_0 = 2.865$ volts: I(t) is spontaneously oscillating at a fundamental frequence $f_1 = 63.4$ kHz. At $V_0 = 2.907$ volts, the system becomes quasiperiodic: a second spectral component appears at $f_2 = 14$ kHz, incommensurate with f_1 [figure 1(b)]. At $V_0 = 2.942$ volts, the system is still quasiperiodic; however, the two modes are interacting and the nonlinear mixing gives spectral peaks at the combination frequencies $f = mf_1 + nf_2$, with m,n integers [figure 1(c)].

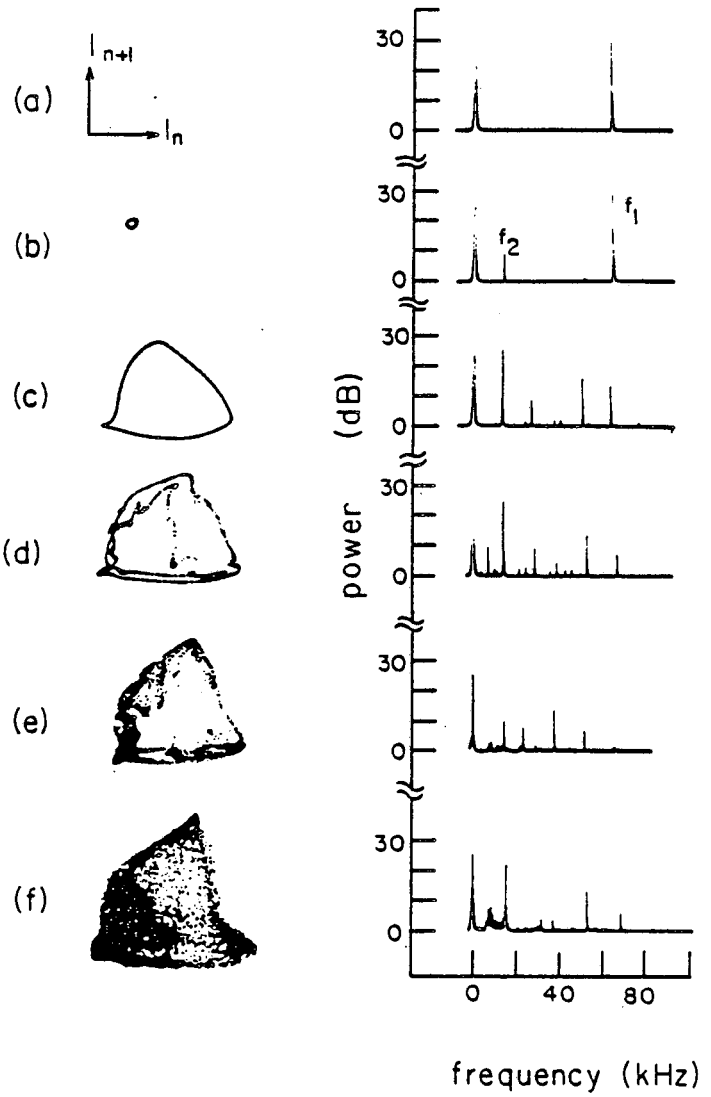

Fig. 1. Return maps, I_n vs. I_{n+1} (where $\{I_n\}$ is the set of local current maxima), and power spectra of the plasma current I(t) at $B_0 = 11.15$ kGauss with increasing V_0: (a) 2.865 volts, periodic at $f_1 = 63.4$ kHz. (b) 2.907 volts, quasiperiodic with second frequency $f_2 = 14$ kHz. (c) 2.942 volts, quasiperiodic with combination frequency components. (d) 3.016 volts, onset of chaos. (e) 3.033 volts, chaotic. (f) 3.058 volts, more chaotic; the fractal dimension of this attractor, $d = 2.7$, is measured in figure 3.

As V_0 in increased further, we observe a series of frequency lockings[10], i.e., (f_1/f_2) = rational number, until the onset of chaos is reached, indicated by a slight broadening of the spectral peaks [figure 1(d)]. As V_0 is increased further, the e-h plasma exhibits increasingly turbulent behavior [figures 1(e) and (f)]. This is followed by a return to quasiperiodicity at $V_0 = 3.125$ volts and, subsequently, simple periodicity at $V_0 = 3.442$ volts.

Figure 1 also shows a sequence of return maps, topologically equivalent to Poincaré sections.[11] Periodic motion corresponds to a closed 1-dimensional orbit in phase space; the Poincaré section in this case is simply a point [figure 1(a)]. Similarly, when the system is quasiperiodic, corresponding to motion on a 2-dimensional torus, the Poincaré section is approximately a circle [figures 1(b) and (c)]. However, as the system becomes chaotic, we find that the Poincaré section begins to wrinkle and to occupy an extended region. This does not *necessarily* imply that the behavior is stochastic, but rather that the dimension of the strange attractor (which is one greater than the dimension of the Poincaré section) is too large to be determined by visual inspection of the Poincaré section. For these attractors the fractal dimension must be calculated quantitatively.

The fractal dimension is a measure of the number of "active" degrees of freedom needed to characterize the evolution of a system. If this evolution is described by trajectories in a G-dimensional phase space, then the fractal dimension d_F is defined as follows:[3]

$$d_F = \lim_{\delta \to 0} \frac{\log M(\delta)}{\log (1/\delta)} \qquad (1)$$

where the phase space has been partitioned into cubes of volume δ^G and $M(\delta)$ is the number of these cubes visited by the attractor.[12] This measure is known variously as the capacity, Hausdorff dimension, and fractal dimension. Other, alternative, dimensions which characterize strange attractors have also been devised. These include the information dimension d_I,[3] and the correlation dimension d_C.[13] It has been proven[14] that generally $d_F > d_I > d_C$. However, in most cases where these dimensions have been calculated, all three have yielded almost identical results.[13,15,16,17]

Equation (1) assumes an attractor contained within a G-dimensional phase space. The coordinates of the phase space may be any set of variables which, when taken together, uniquely identify the state of the system. For our experiments, these variables could be the plasma density and momentum measured at many different points within the crystal (provided of course that the number of independent probes G were greater than the fractal dimension d). Experimentally, this method of characterizing the system is difficult to realize. It is not always feasible to have an arbitrary number of probes for a given system and, further, it is not known how many probes will be required. One cannot know this until the fractal dimension d_F has already been

determined.

Fortunately, there is a method of reconstructing phase space from a single dynamical variable using a technique based on the embedding theorem.[1,13,15,18] If $\{V_1(t), V_2(t), \ldots, V_G(t)\}$ is a phase space constructed from G independent variables, then the reconstructed phase space $\{V_1(t), V_1(t+\tau), \ldots, V_1(t+(D-1)\tau)\}$ is conjectured to be topologically equivalent to the original phase space, for almost all τ, provided $D > 2G+1$.[18] Attractors in both the original and reconstructed phase spaces will be characterized by the same Lyapunov exponents and fractal dimensions. In our experiments, we use a reconstructed phase space derived from the measured current I(t). The coordinates of our phase space are thus $\{I(t), I(t+\tau), \ldots, I(t+(D-1)\tau)\}$, where, typically, $5\,\mu s < \tau < 15\,\mu s$; we find that the calculated fractal dimensions are independent of τ. In practice, one calculates the fractal dimension d for increasing embedding dimension D until d converges with respect to D.

Calculations of fractal dimensions using the box-counting algorithm of Eq. (1) tend to be computationally inefficient.[19] Large regions of phase space are visited only rarely. Thus large numbers of data points and, consequently, large amounts of computer time are often required. Calculations on systems with $d \approx 3$ can require more than a million data points. However, it is possible to calculate the "pointwise" fractal dimension[20] (which is conjectured[3] to be equal to the information dimension) using the following, more efficient algorithm.[21] A D-dimensional phase space is reconstructed from a single dynamical variable. Next one computes the number of points on an attractor, $N(\epsilon)$, which are contained within a D-dimensional hypershpere of radius ϵ centered on a randomly selected point on the attractor. One expects scaling of the form:

$$N(\epsilon) \propto \epsilon^d \tag{2}$$

where d is the fractal dimension of the attractor. Thus a plot of $\log N(\epsilon)$ vs. $\log \epsilon$ is expected to have slope d (for sufficiently small ϵ). This procedure is carried out for consecutive values of $D = 2, 3, 4, \ldots$, until the slope has converged. This is done to insure that the embedding dimension chosen is sufficiently large (important if the dimension of the phase space is not known) and to discriminate against high dimensional stochastic noise, not of known deterministic origin.

A comparison of equations (1) and (2) illustrates the difference between the fractal and pointwise dimensions. The calculation of the fractal dimension involves determining the fraction of phase space occupied by the entire attractor. On the other hand, the pointwise dimension is defined as the scaling of $N(\epsilon)$ with ϵ, for $N(\epsilon)$ centered around a *single* point on the attractor. The conjecture that the pointwise dimension is equal to the information dimension (which, like the fractal dimension, is measured globally over the

attractor[3]) implies that the scaling laws which govern the fractal structure are constant throughout the attractor. It is therefore sufficient to determine the scaling exponent at a single point on the attractor. We note that the pointwise dimension is conjectured to be equal to the information dimension, not the fractal dimension, but, as mentioned earlier, the two are found to be experimentally indistinguishable.

We have computed the pointwise dimension d for our plasma instabilities at various points along the quasiperiodic transition to chaos described above. For each of eleven values of V_0 between 2.865 volts and 3.125 volts ($B_0 = 11.15$ kGauss) we recorded N (≈ 98000) successive values of the current at 5 μs intervals [i.e., $I_n = I(t+n\tau)$, $n = 1, \ldots, 98000$; $\tau = 5\,\mu s$]. From each data set $\{I_1, \ldots, I_N\}$ we constructed $N - D + 1$ vectors $G_n \equiv (I_n, I_{n+1}, \ldots I_{n-D+1})$ in a D-dimensional phase space. In principle, one should be able to calculate the fractal dimension with Eq. (2) using data centered around a single point on the attractor G_n; that is, calculations of $N(\epsilon)$ centered around different vectors G_i should all yield the same value of d. Experimentally this is not actually observed, as discussed below.

For $V_0 = 3.058$ volts we constructed plots of $\log N(\epsilon)$ vs. $\log\epsilon$ for $N(\epsilon)$ centered on 27 randomly selected vectors G_i. The slopes of these 27 plots comprise 27 measurements of the fractal dimension d. A histogram of these values of d is shown in figure 2(a); the result is a distribution centered around $d = 2.4 - 2.6$. However, a careful examination of the 27 plots of $\log N(\epsilon)$ vs. $\log\epsilon$ indicates that several of these plots yield unreliable values of d, for reasons discussed below. Upon elimination of these suspect points, the width of the histogram narrows appreciably, as shown in figure 2(b). For an experimental system, there are at least three conditions under which one will not expect scaling of the form of Eq. (2) for $N(\epsilon)$ centered around certain random points on the attractor.

First, the random point may be situated in a region of the attractor which is visited only rarely. Thus, even with a large number of data points there are not enough nearby data points to resolve the fractal structure and thus to observe the scaling of Eq. (2). In such a case, the plot of $\log N(\epsilon)$ vs. $\log\epsilon$ will have a gradually increasing slope for small ϵ, in contrast with the break to a steeper, non-convergent slope for small ϵ that is expected for chaotic systems in the presence of thermal noise.[22] This break is expected because the dynamics of all physical systems are characterized by thermal (stochastic) processes at energies below $\sim kT$; these processes are characterized by fractal dimensions on the order of the number of particles in the system.[23] We eliminate all plots which do not show the physically expected break to steeper slope for small ϵ.

A second difficulty arises when $N(\epsilon)$ is centered in a region of the

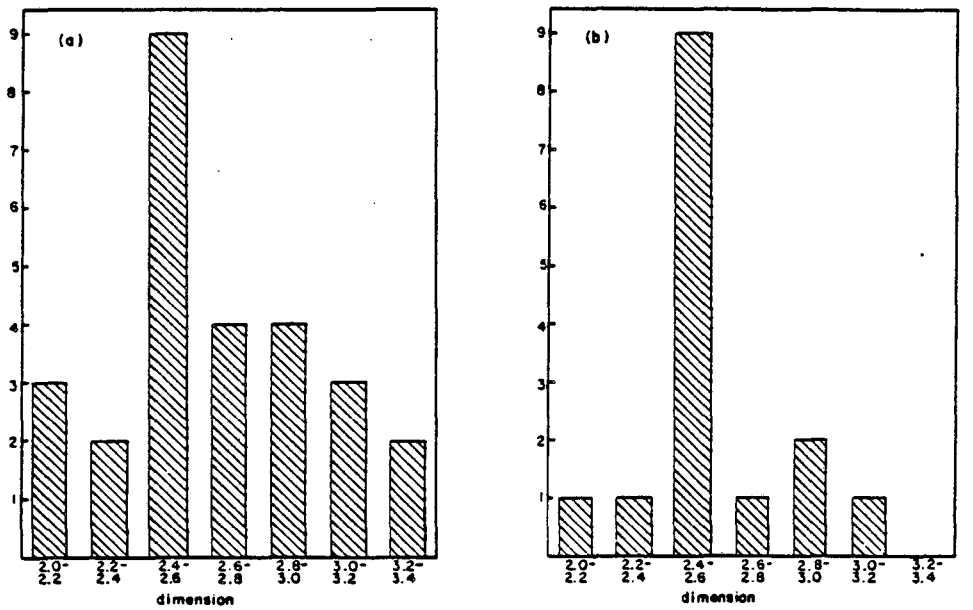

Fig. 2. Histogram of fractal dimension calculations for $V_0 = 3.058$ volts and $B_0 = 11.15$ kGauss [same operating conditions as in figure 1(f)]. (a) The fractal dimension is calculated 27 times by observing the scaling of $N(\epsilon)$ [equation (2)] around 27 randomly chosen points in reconstructed phase space. The vertical axis refers to the number of these calculations for which the fractal dimension d is found to be in each of the ranges specified on the horizontal axis. The distribution is centered around $d = 2.4 - 2.6$. (b) The same distribution as (a), except that those calculations yielding unphysical results (see text) have been removed. The distribution is still centered at $d = 2.4 - 2.6$, but it has narrowed appreciably.

attractor where the length scales over which the structure is fractal are comparable to or less than those corresponding to thermal fluctuations ($\sim$kT). In these cases the fractal structure may be "washed out" by thermal noise, resulting in a plot of $\log N(\epsilon)$ vs. $\log\epsilon$ which does not have a well defined (convergent) slope. We discard these plots as well.

Finally, if a hypershpere $N(\epsilon)$ is centered on the attractor in a region of high lacunarity,[24] the resulting plot of $\log N(\epsilon)$ vs. $\log\epsilon$ will not have a well defined slope.

By rejecting those plots of $\log N(\epsilon)$ vs. $\log\epsilon$ which do not exhibit physically reasonable characteristics (i.e., a well defined slope and a break to steeper slope for small ϵ), we obtain a much sharper distribution of values for the fractal dimension d, as seen in figure 2(b). However, when we plot $\log\overline{N(\epsilon)}$ vs. $\log\epsilon$, where $\overline{N(\epsilon)}$ is the average over many hyperspheres, we find that this average slope is unchanged ($\pm 5\%$) by the rejection of the unphysical plots. This was found to be true for several cases. Thus, in most instances we simply plot $\log\overline{N(\epsilon)}$ vs. $\log\epsilon$ for $\overline{N(\epsilon)}$ averaged over many randomly chosen hyperspheres. (This same procedure has also been utilized in studies of free surface modes of a vertically forced fluid layer[25] and Couette-Taylor flows.[15]) Figure 3(a) shows our results for $V_0 = 3.058$ volts with the embedding dimension $D = 2,4,6$, and 8; for $D \geq 6$ the slope (and thus the fractal dimension) has converged to 2.7. The fractal dimension for all the states shown in figure 1, as well as several states not shown, are plotted in figure 3(b).

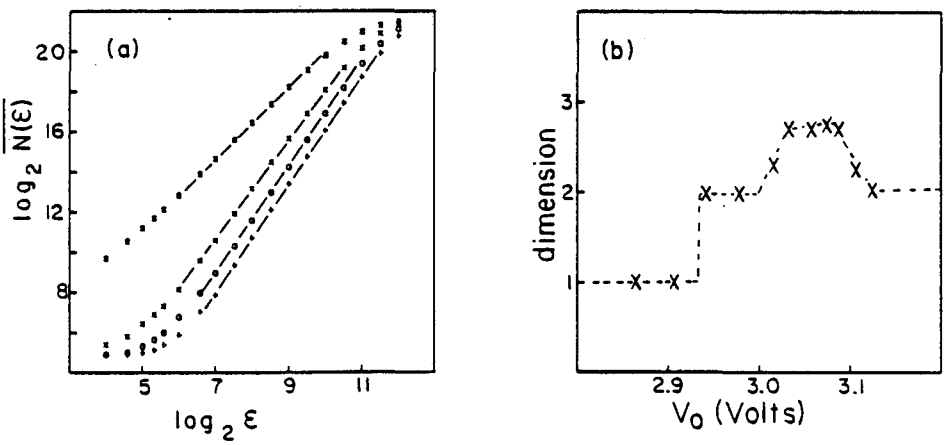

Fig. 3. (a) Plots of $\log\overline{N(\epsilon)}$ vs. $\log\epsilon$ used to determine the fractal dimension d of the chaotic attractor at $V_0 = 3.058$ volts, $B_0 = 11.15$ kGauss, using method discussed in text and Eq. (2) [averaged over 25 randomly chosen points in reconstructed phase space]. Embedding dimension $D = 2, 4, 6$ and 8 correspond, respectively, to symbols *, x, o and +; for $D \geq 6$, the slope converges to $d = 2.7$. (b) Dependence of measured dimension d on applied voltage V_0. $B_0 = 11.15$ kGauss. Values $d = 1$ and $d = 2$ correspond to periodic and quasiperiodic orbits, respectively. All calculations were checked for convergence with respect to embedding dimension D and number of data points sampled N. All values of d represent an average over 25 randomly selected points in reconstructed phase space.

Within the chaotic regime, the fractal dimension of the attractor varies between 2 and 3. This demonstrates that the observed plasma turbulence shown in figures 1(d)-(f) may be described with only a few degrees of freedom; the behavior of the system remains largely deterministic. If the observed turbulence were due to thermal or stochastic processes, then a measurement of the fractal dimension d would not have converged for small embedding dimension D. The dimension of the attractor d could then have been on the order of the number of conduction electrons and holes in the crystal[23] ($\approx 10^{10}$).

4. Transitions to "Strong" Turbulence

With sufficiently large applied electric and magnetic fields, we find that we can drive the plasma into a turbulent state from which it will not become periodic again as V_0 is increased further. Instead, all of the frequency peaks in the power spectrum merge into a single, broad, noiselike band. We classify this as a transition to "strong" turbulence. Such a transition is shown in figure 4. At $V_0 = 10.4$ volts, I(t) is simply periodic at $f_0 = 321$ kHz, with higher harmonics present as well [figure 4(a)]. At $V_0 = 11.6$ volts, I(t) is quasi-periodic and at $V_0 = 12.1$ volts (not shown), the onset of broadband "noise" can be observed. At $V_0 = 13.8$ volts [figure 4(b)], only a few of the peaks can be seen above the noise, and when $V_0 = 21.8$ volts [figure 4(c)], only a very broad peak remains.

We find that this transition to strong turbulence is characterized by a partial loss of spatial coherence. In the right hand column of figure 4, we plot the voltage traces across two pairs of probe contacts which are separated by $r = 4$ mm, for $V_0 = 10.4$, 13.8, and 21.8 volts. In the periodic case, the wave is spatially coherent with a wavelength of approximately 8 mm (i.e., a 4 mm separation corresponds to a 180° phase shift). At $V_0 = 13.8$ volts we are just beyond the onset of the break-up of spatial order -- the basic oscillatory pattern and the 180° phase shift are approximately maintained between the two traces, but changes in the shapes and spacings of the peaks can also be observed. For $V_0 = 21.8$ volts, the wavelike structure of the traces, as well as the readily observable spatial correlation, is no longer present.

We would like to determine whether this breakup of spatial order can be characterized by chaotic dynamics: Do the spatially uncorrelated states still correspond to motion in phase space along a low-dimensional strange attractor? We have as yet been unable to answer this question definitively. Just prior to the breakup of spatial coherence, $V_0 = 12.1$ volts, the total current I(t) of the system is characterized by a low-dimensional attractor; measurements of the fractal dimension yield $d = 2.5$ [figure 5(a)]. However, just after the onset of spatial disordering, $V_0 = 12.9$ volts, the fractal dimension has

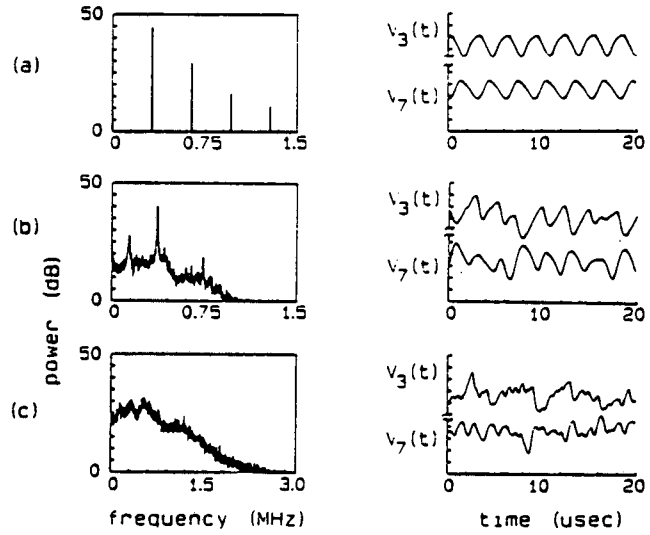

Fig. 4. Left, measured power spectra of I(t); right, measured voltages for two pairs of probe contacts separated by r = 4 mm: $V_3(t)$ and $V_7(t)$ correspond to probe pairs located 3 and 7 mm away from the p^+ contact, respectively. $B_0 = 11.15$ kGauss. (a) $V_0 = 10.4$ volts, periodic at $f_0 = 321$ kHz. At $V_0 = 12.1$ volts (not shown) temporal chaos has set in, with measured fractal dimension $d \approx 2.5$, figure 5(a). (b) $V_0 = 13.8$ volts, power spectrum has broad base and peaks; comparison of $V_3(t)$ and $V_7(t)$ shows beginning of spatial incoherence; measured fractal dimension $d > 8$. (c) $V_0 = 21.8$ volts, power spectra very broad, more marked loss of spatial coherence, measured fractal dimension $d > 8$.

increased to the point where we cannot calculate its value – we can only set a lower limit: $d \geq 8$. This is shown in figure 5(b) where the slope has not converged with respect to either embedding dimension D or number of data points N. Figure 5(b) was taken with N = 884000 and required 50 hours of CPU time on a Sun microcomputer. For $V_0 = 21.8$ volts, N = 884000 points and embedding dimension D = 18, the slope is 14 and has definitely not converged.

For our fractal dimension plots of figure 5 we note that the curves become horizontal (saturate) for (i) $\epsilon > \epsilon_1$, a hypershpere large enough to include all points on the attractor and for (ii) $\epsilon < \epsilon_2$, a hypersphere so small that only the single point at its center is within it. This behavior is to be

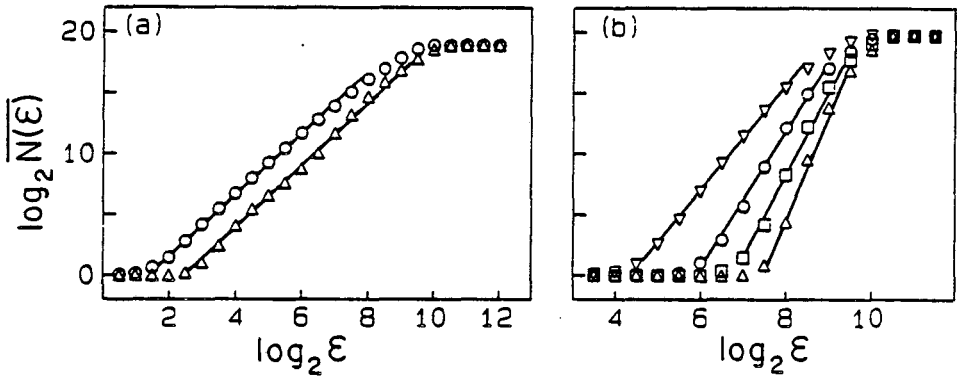

Fig. 5. Plots of $\log\overline{N(\epsilon)}$ vs. $\log\epsilon$ used to determine fractal dimension d at $B_0 = 11.15$ kGauss. (a) $V_0 = 12.1$ volts, $N = 490000$ data points; the symbols o and Δ refer to embedding dimensions D of 4 and 8, respectively. Slopes have converged to 2.5 with respect to both D and N. (b) $V_0 = 12.9$ volts, $N = 884000$; ∇, o, $\square$, and Δ refer to $D = 6$, 10, 14 and 18, respectively. Slopes have not converged with respect to either D or N. For $D = 18$ slope is 8.7.

expected for all fractal dimension plots, provided ϵ is varied sufficiently; it is important to do this to ensure that all experimental data are examined.

Calculations based on time series taken across different pairs of probe contacts $V_i(t)$ yield the same fractal dimensions d as those based on total current I(t), for both spatially coherent and incoherent states. Further, we find that for fixed values of our applied fields, the power spectrum measured across a pair of probe contacts $|V_i(\omega)|^2$ is essentially identical to the power spectrum of the total current $|I(\omega)|^2$. This suggests that the spatial incoherence may be due to the dispersive nature of the e-h plasma.

This difficulty in calculating large fractal dimensions is a problem incurred with very chaotic systems. The number of data points required for convergence increases exponentially with the fractal dimension of the system.[19,26] At present, although we know that our system experiences a large jump in dimensionality at the onset of spatial incoherence, we have not yet determined whether this onset is characterized by chaotic dynamics of an attractor of fractal dimension may orders of magnitude smaller than the number of degrees of freedom of the particles in the system ($\sim 10^{10}$). Other approaches for quantitatively characterizing very chaotic states (say, $d > 10$) will need to be developed before this intriguing question can be answered.

We wish to thank E. E. Haller and the members of his laboratory for the Ge samples and assistance in the sample preparation. This work was supported by the Director, Office of Energy Research, Office of Basic Energy Science, Materials Science Division of the U. S. Department of Energy under Contract No. DE-AC03-76SF00098.

References

1. for example, H. L. Swinney: Physica (Utrecht) **7D**, 3 (1983); see also *The Physics of Chaos and Related Problems*, edited by S. Lundqvist, Phys. Scr. **T9** (1985).
2. D. Ruelle and F. Takens: Comm. Math. Phys. **20**, 167 (1971); E. Ott: Rev. Mod. Phys. **53**, 655 (1981).
3. for example, J. D. Farmer, E. Ott, J. A. Yorke: Physica (Utrecht) **7D**, 153 (1983).
4. A. Wolf, J. B. Swift, H. L. Swinney and J. A. Vastano: Physica **16D**, 285 (1985).
5. J. P. Crutchfield and N. H. Packard: Int. J. Theor. Phys. **21**, 433 (1982); Physica **7D**, 201 (1983); P. Grassberger and I. Procaccia: Phys. Rev. A **28**, 2591 (1983).
6. I. L. Ivanov and S. M. Ryvkin: Zh. Tekh. Fiz. **28**, 774 (1958) [Sov. Phys. Tech. Phys. **3**, 722 (1958)].
7. C. E. Hurwitz and A. L. McWhorter: Phys. Rev. **134**, A1033 (1964).
8. G. A. Held, C. Jeffries and E. E. Haller: Phys. Rev. Lett. **52**, 1037 (1984); *Proceedings of the Seventeenth International Conference on the Physics of Semiconductors, San Francisco, 1984*, edited by D. J. Chadi and W. A. Harrison (Springer-Verlag, New York, 1985), p. 1289.
9. G. A. Held and C. Jeffries: Phys. Rev. Lett. **55**, 887 (1985).
10. for example, J. P. Gollub and S. V. Benson in *Pattern Formation and Pattern Recognition* edited by H. Haken (Springer-Verlag, Berlin, 1979), p. 74.
11. N. H. Packard, J. P. Crutchfield, J. D. Farmer and R. S. Shaw: Phys. Rev. Lett. **45**, 712 (1980).
12. Unconventional notation is used in Eq. (1) to avoid confusion with the notation of Eq. (2).
13. P. Grassberger and I. Procaccia: Phys. Rev. Lett. **50**, 346 (1983).

14. H. G. E. Hentschel and I. Procaccia: Physica 8D, 435 (1983).

15. A. Brandstäter *et al.*: Phys. Rev. Lett. **51**, 1442 (1983).

16. H. L. Swinney and J. P. Gollub: to appear in Physica D.

17. This has been observed in calculations of fractal, information and correlation dimensions for a system consisting of a driven p-n junction in series with an inductor and a resistor. G. A. Held and C. Jeffries, unpublished.

18. F. Takens: "Detecting Strange Attractors in Turbulence", in *Lecture Notes in Mathematics 898*, edited by D. A. Rand and L. S. Young (Springer-Verlag, Berlin, 1981), p. 366.

19. H. S. Greenside, A. Wolf, J. Swift and T. Pignaturo: Phys. Rev. A **25**, 3453 (1982).

20. The pointwise dimension is defined in reference 3. Similar definitions of dimension have been given in references 11, 20, 21, and 31 therein.

21. This is the method used by A. Brandstäter *et al*, in reference 15. See also reference 13.

22. A. Ben-Mizrachi, I. Procaccia and P. Grassberger: Phys. Rev. A **29**, 975 (1984).

23. A fractal dimension of this magnitude ($\sim 10^{10}$) is experimentally unattainable for two reasons. First, an inordinate number of data points would be required, as discussed in Section 4. Second, one would need to measure signals with a very large bandwidth $\Delta f \sim 1/\tau$, where τ is the shortest fluctuation time; typically $\Delta f \sim 10^9 - 10^{14}$ Hz for stochastic noise in conducting media. Thus, fractal dimensions of this magnitude are operationally meaningless.

24. B. B. Mandelbrot: *The Fractal Geometry of Nature* (W. H. Freeman and Company, New York, 1983), p.310.

25. S. Ciliberto and J. P. Gollub: J. Fluid Mech. **158**, 381 (1985).

26. H. Froehling, J. P. Crutchfield, J. D. Farmer, N. H. Packard, and R. Shaw: Physica **3D**, 605 (1981).

LAWRENCE BERKELEY LABORATORY
TECHNICAL INFORMATION DEPARTMENT
UNIVERSITY OF CALIFORNIA
BERKELEY, CALIFORNIA 94720